

Selection Effects and Robust Measures of Galaxy Evolution

Henry C. Ferguson

Space Telescope Science Institute, Baltimore, MD 21218

ferguson@stsci.edu

ABSTRACT

A variety of subtle, and not-so-subtle selection effects influence the interpretation of galaxy counts, sizes and redshift distributions in the Hubble Deep Field. Comparison of the different HDF catalogs available in the literature and on the world-wide-web reveals generally good agreement, although the effects of different isophotal thresholds and different splitting algorithms are readily apparent. As the basic source detection and photometry algorithms are similar for the different catalogs, the selection effects are likely to affect them all.

Through simulations, we explore the utility of image moments for inferring the true sizes of galaxies. The truncation of galaxy profiles at a fixed isophote has serious consequences, which limit constraints on the size distribution to galaxies with isophotal magnitudes $I_{814} < 27.5$. Present-day L^* spirals would be undetected in the HDF above redshifts $z \approx 1.2$, and present-day ellipticals would disappear at $z \approx 1.8$.

The Lyman break provides a way to identify high-redshift galaxies at very faint magnitudes. However, galaxies that are at redshifts high enough to vanish from the HDF F300W or F450W filters also suffer severely from photometric biases. For example, at fixed total apparent magnitude and physical scale length, a galaxy at $z = 4$ will have a mean surface brightness 1.2 mag fainter than a galaxy at $z = 2.75$. This lower surface brightness will result in an apparent decrease in the number density of objects, and the inferred luminosity density, even for models where there is no intrinsic evolution. We illustrate the effects of these biases on the estimates of the number of Lyman “dropouts” in the HDF and on the luminosity density at $z > 2$.

Introduction

In trying to decipher the origin of galaxies from a collection of fuzzy patches on the sky, we must keep in mind that even the Hubble Deep Field, with its exquisite depth and

resolution, provides a distorted view of the universe at large. This view is distorted by the fact that we are looking only at optical wavelengths, which for the most part probe the rest-frame ultraviolet portion of the spectra of the galaxies of interest. It is distorted by the fact that the background noise of the detector limits detection of galaxies to those that exceed a certain threshold over a certain number of pixels: faint extended objects are extremely difficult to detect; galaxies with multiple peaks in their light distribution may appear as separate objects. It is distorted by the fact that many of the galaxy images overlap, making it difficult to separate one galaxy from the next. Finally, it is distorted by physical effects such as obscuration by dust or gravitational lensing. These effects of dust and lensing are amply discussed in this conference by Madau, Meurer, Rowan-Robinson, Blandford, and others. I will focus on the selection effects, seeking to explore and quantify some of the concerns that have colored many of the discussions of the HDF and other deep galaxy surveys.

HDF Catalogs

In making the HDF data set non-proprietary, one of the hopes was that different groups would be stimulated to reduce and analyze the data independently with different scientific objectives and different algorithms. To some extent this has happened. The data have been largely reprocessed by several different groups (Flynn, Gould, & Bahcall 1996; Ratnatunga 1996), and different techniques have been used for source detection and photometry (Williams et al. 1996; Lanzetta, Yahil, & Fernandez-Soto 1996; Elson, Santiago, & Gilmore 1996; Couch 1996; Metcalfe et al. 1996). As much of the discussion at this meeting is focused on comparing what we see in the HDF to what we expect from models of galaxy evolution, it is worth examining some of these catalogs to see how well they agree with each other, and how well they reproduce our own preconceptions of how sources should be counted.

For this purpose, I have chosen four catalogs that have been used in HDF publications. All the catalogs have in common the feature that they convolve the data to smooth the noise over a scale relevant to the sources being sought, and then mark as sources those objects that have a certain number of connected pixels more than some multiple of the rms background fluctuations. This procedure is equivalent to Wiener filtering with a Gaussian source model, and is optimal in the least-squares sense for detecting unresolved objects against a random, uncorrelated background. It is not so clearly optimal for finding galaxies in an image where galaxies have a wide range of sizes and have isophotes that in many cases overlap. However, to my knowledge there have not been any HDF catalogs based, for

example, on wavelets or on median filtering over a variety of scales, which might have a different set of selection effects.

Completeness

The catalogs are briefly summarized in Table 1, which lists the software package used, the number of objects found, and the rough detection criteria. The total source counts are influenced primarily by the isophotal threshold. To a certain extent it is a matter of taste how deeply to push into the noise. The Metcalfe et al. (1996) catalog is the deepest (or least conservative) while the Lanzetta, Yahil, & Fernandez-Soto (1996) catalog is the shallowest (or most conservative). While the total number of sources varies by more than a factor of two between the catalogs, down to $V_{606} = 27.8$ the counts in the different catalogs agree to within 20% of the mean.

Object splitting and merging

A variety of schemes have been developed for splitting up sources that have multiple peaks above the detection isophote into separate “parent” and “daughter” objects. There is no mathematical rigor in these techniques. Identification of daughter objects is typically done by passing successively higher isophotal thresholds over the image and making lists of sources within sources. Different algorithms are then used to “merge” the various pieces back into objects that are likely to be part of the same galaxy. Williams et al. (1996) use color information to help with this merging; in other cases the decisions were made using information from one band.

The differences in how subcomponents are counted are illustrated in the sections of the F606W image shown in Figs. 1-4, where we show the positions of galaxies with total magnitudes brighter than 28.5 from the four different catalogs. Broadly speaking, the Lanzetta, Yahil, & Fernandez-Soto (1996) catalog tends to do the least splitting of objects within common isophotes, while the Metcalfe et al. (1996) catalog does the most splitting. There are many cases, such as the peculiar galaxy just to the right and above the center of the images, where it is not at all obvious how one should count. Even more problematical is the object that looks like a late-type spiral which is superimposed on the outer isophotes of a bright elliptical galaxy near the bottom of the frame. In the Lanzetta, Yahil, & Fernandez-Soto (1996) catalog, this object is counted as part of the elliptical. In the Couch (1996) catalog, it is counted as four objects. It is counted as five by Williams et al. (1996)

and 4-6 by Metcalfe et al. (1996).

From an analysis of the angular correlation function in their HDF catalog (constructed using DAOFIND), Colley et al. (1997) suggest that such difficulties lead to an overestimate in the number of faint galaxies by a factor of 2.5. While this estimate strictly applies only for the subset of 196 color-selected high-redshift candidate objects in their catalog, such overcounting is likely to be true at some level for galaxies at all redshifts in all the catalogs. However, two important facts mitigate the effect of this problem on the interpretation of deep galaxy counts. The first is that the oversplitting of some objects is counteracted by the overmerging of others. That is, many close projections of unrelated objects are counted as one object. This effect can be quantified by simulations. Second, because the artificial splitting of large galaxies into several smaller ones preserves the total luminosity, the effect shifts the number counts both vertically and horizontally in such a way that the predictions of models are not greatly affected. Figure 5 shows the effect of overcounting for a non-evolving model with $q_0 = 0.01$. We have assumed here that galaxies at $I_{814} = 22$ are counted on average as three objects, and that the overcounting decreases with magnitude such by $I_{814} = 30$ objects are counted only once.

“Total” magnitudes

Different photometry packages use different techniques to estimate total magnitudes. These estimates are based on extrapolations of galaxy sizes or surface brightnesses below the initial isophotal limits of detection, and face serious difficulties in the particular cases of overlapping galaxies. Even for isolated galaxies, the reliance on the initial estimates for galaxy sizes and/or surface brightness profiles can introduce serious biases for galaxies near the detection threshold. Nevertheless, before addressing the potential biases, it is interesting to compare the results from the different catalogs.

Brighter than $V_{606} = 28$, magnitudes from the different catalogs agree reasonably well. Even if the photometry were in principle perfect, the different splitting algorithms would introduce some scatter at bright magnitudes. Figure 6 shows comparisons between the Williams et al. (1996), Metcalfe et al. (1996), and Couch (1996) magnitudes. The total magnitudes agree to within 0.5 mag rms over the full magnitude range. There is a systematic trend for the Metcalfe et al. magnitudes to be brighter than the Williams et al. mags. The difference increases toward faint mags, and is as much as 0.3 mag at $V_{606} = 28$. The systematic differences between Couch and Williams et al. catalogs are less than 0.15 mag. The good agreement between catalogs suggests that the different photometry packages all do more-or-less the same thing. The discussion of the selection biases below, which

focuses specifically on the Williams et al. (1996) catalog, is thus likely to apply to all the catalogs.

Galaxy radii

Figure 7 shows the distribution of first-moment radii of galaxies from the Williams et al. HDF catalog and the Medium Deep Survey (Ratnatunga, Griffiths, & Ostrander 1997).¹ These isophotal radii keep decreasing right down to the detection limits of the survey. At $V_{606} = 27$ the typical first-moment radius corresponds to less than 2 kpc for *any redshift*, for cosmologies with $q_0 > 0$. The first-moment radius is defined as

$$r_1 = \sum rI(x, y) / \sum I(x, y), \quad (1)$$

where $I(x, y)$ is the intensity in each pixel. The quantity $R_k = 2r_1$ is often referred to as the “Kron radius”. Kron (1978) showed that in typical ground-based surveys the radius R_k typically encompasses 90% of the light from an object. If the intensity could be measured precisely over the entire galaxy, the relations between first-moment radii and scale radii would be $r_1 = 2\alpha = 1.19r_e$ for spirals, and $r_1 = 2.28r_e$ for ellipticals. The size–magnitude relations for non-evolving L^* ellipticals and spirals are shown in Fig. 7, for two values of q_0 .

Taken at face value, the steep radius–magnitude relation implies that faint galaxies are intrinsically very compact. However, r_1 is computed using pixels above the isophotal threshold, and thus is subjected to severe biases as we approach the limiting magnitude of the survey. These biases enter in several ways: (1) because of isophotal selection, at fixed total magnitude larger galaxies will preferentially disappear from the sample; (2) near the detection limit of the survey the first-moment radius r_1 becomes progressively biased toward smaller values; and (3) near the detection limit, total magnitudes computed either from Kron magnitudes or from the flux within some multiple of the isophotal area become progressively biased toward faint values. While effects (2) and (3) can be partially controlled by measuring Petrosian (1976) radii and magnitudes, isophotal selection effects inevitably bias the sample of galaxies selected for such measurements.

We can quantify these selection effects by creating simulated images with the same noise properties as the HDF images and running them through the same source detection

¹ The Medium Deep Survey (MDS) catalog is based on observations with the NASA/ESA Hubble Space Telescope, obtained at the Space Telescope Science Institute, which is operated by the Association of Universities for Research in Astronomy, Inc., under NASA contract NAS5-26555. The Medium-Deep Survey is funded by STScI grant GO2684.

and photometry routines. The best way to do this would be to add a small number of galaxies to the HDF image itself and reprocess it hundreds of times. However, for the purpose of this conference I have taken the shortcut of constructing only two simulated images, one with face-on exponential disks and the other with deVaucouleurs profiles. The galaxies have magnitudes between 25 and 30 and a range of scale lengths. The images are somewhat less crowded than the real HDF, so crowding should not affect the results much. In any case, the results here are meant to be indicative rather than definitive. The noise was simulated as described by Ferguson & Babul (1998), and the source detection and photometry were done using the same version of FOCAS with the same parameters used by Williams et al. (1996).

Figure 8 shows the selection boundary for galaxies with exponential profiles (left panel) and deVaucouleurs profiles (right panel). The numbers in the figure give the fraction of the input sample of galaxies recovered as a function half-light radius r_e and total magnitude, I_{814} . The solid curves show the limits of the survey expected from the rms sky noise of the HDF images, assuming FOCAS detects sources with AB magnitude $I_{814} < 30.6$ within a radius of $0.064''$. This seems to be a reasonably good model of the 50% completeness limit of the Williams et al. catalog. To put this in context, the dashed curves show the size–magnitude relation for non-evolving L^* galaxies. A typical present day spiral would drop below the selection limits of the survey by $z = 1.2$, even though its total magnitude is brighter than $I_{814} = 28$ out to $z = 2.5$. A typical elliptical would be invisible beyond $z = 1.8$.

Figure 8 illustrates the point that the HDF and other deep surveys should not be treated as flux-limited surveys. The sizes of galaxies matter as much as their total luminosities. This fact, although well known, is often ignored in comparing model counts to the data. With the HDF and future surveys it is extremely important to take this into account.

Robust constraints on galaxy sizes

Of course, it would be nice if we could infer something robust about the physical sizes of galaxies in the HDF, independent of any assumed model. To do this, we must translate the selection boundaries in Figure 5 from the theoretical M_{tot}, r_e plane, to the observed M_{iso}, r_1 plane. This can be done analytically or numerically for the different profiles, and can also be done empirically from the FOCAS measurements of the simulated galaxies. Figure 9 shows the translated curves from Fig. 8, along with the observed distribution of sizes and magnitudes of galaxies in the HDF. The thin lines show the fiducial galaxies from

Fig. 8.

Brighter than $I_{814} = 27.5$, the locus of points clearly peaks at values of r_1 that are well away from the selection boundary. Hence it is probably safe to assume that the relatively compact sizes and high surface brightnesses of the HDF galaxies are a real phenomenon, and not an artifact of galaxy selection. The apparent sizes are smaller than those of present-day L^* disk-dominated spirals, but not significantly smaller than those of luminous ellipticals. Very little can be said about the intrinsic sizes of galaxies fainter than $I_{814} = 27.5$, because it is likely that many galaxies are missed due to low surface brightness. The survey limit determines the upper bound on r_1 , and the PSF determines the lower bound. This truncation of the survey by the isophotal limit means that galaxy counts fainter than $I_{814} = 27.5$ must also be viewed as a lower limit. Also large corrections are required to translate from FOCAS isophotal to true total magnitudes near the survey limit. Such corrections can be derived for models, but cannot be derived with any certainty from the data themselves.

Lyman Break Galaxies

The past two years have brought an explosion in the number of star-forming galaxies identified at redshifts $z > 2$. The HDF has contributed to this by providing a set of robust high-redshift galaxy candidates several magnitudes below the detection limits of current Keck spectroscopy. Madau et al. (1996) used the statistics of Lyman-break objects in the HDF to estimate the luminosity-density in redshift intervals centered at $\langle z \rangle = 2.75$ and $\langle z \rangle = 4$. Together with constraints from the CFRS survey (Lilly et al. 1995) and a local $H\alpha$ survey (Gallego et al. 1995), this analysis provides an indication of the metal-formation rate and integrated star-formation rate as a function of redshift. Because it puts the observations in a physical context, the “Madau diagram” has become a popular foil for discussing and testing models of galaxy formation, and has been subject to a fair amount of scrutiny. Much of the debate centers on how much dust there is in star-forming galaxies at high redshift, and on what corrections are needed for extinction and for galaxies that are too dusty to detect (see contributions by Madau, Rowan-Robinson, and Meurer in this conference). The luminosities of the $\langle z \rangle = 2.75$ and the $\langle z \rangle = 4$ samples are computed at essentially the same rest-frame wavelengths ($\sim 1500 \text{ \AA}$), and thus are probably subject to the similar amounts of extinction. If anything the extinction should be less on average for the $\langle z \rangle = 4$ sample, since there is likely to be less dust at high redshift. This suggests that the decreasing luminosity density from $z = 2.75$ to $z = 4$ is a real effect, indicative of a change in the overall star-formation rate of the universe.

However, it is important to keep in mind that the Lyman break objects, like all other galaxies in the HDF, are selected above a fixed isophote, and are subject to the same selection effects. For example, at fixed total apparent magnitude and physical scale length, a galaxy at $z = 4$ will have a mean surface brightness 1.25 mag fainter than a galaxy at $z = 2.75$. If the Lyman-break objects fall near the selection boundary, this change in surface brightness could in principle translate to a 0.5 dex change in the inferred luminosity density, which is roughly what is observed between these two redshifts.

To explore this effect, we have examined the statistics of Lyman Break galaxies in the models of Ferguson & Babul (1998), comparing what would be derived from an ideal survey, to what we derive from simulated images of the HDF. Figure 10 shows position of model galaxies in Madau et al. (1996) color-color plot. For this figure, the total magnitudes of the galaxies from the models are used, and we have truncated the sample at $I_{814} = 27.6$, which corresponds to the $\sim 10\sigma$ detection limit of the HDF. The Madau et al. (1996) selection criteria applied to this sample yields a total of 62 “U dropouts” and 232 “B dropouts” (compared to 69 and 14, respectively, in the real HDF).

Figure 11 shows FOCAS measurements *of the same model* from simulated images. This figure should be directly comparable to those in Madau et al. (1996). The color selection criteria yield 10 U dropouts and 21 B dropouts. This illustrates the potential severity of the selection effects on the statistics of Lyman break objects. The number density of Lyman-break objects in the input model differs from the number recovered by FOCAS by roughly one order of magnitude!

The effect on the inferred luminosity density is much less severe, but is still quite significant, at least for the models we have tested. Table 2 shows the total magnitude (from the summed flux of all the detected galaxies) and derived metal-formation rates $\dot{\rho}_Z$ (in units of $M_{\odot} \text{ yr}^{-1} \text{ Mpc}^{-3}$) for Lyman-break galaxies selected directly from the model, from the simulated images, and from the real HDF. Isophotal selection decreases the inferred metal-formation rate by a factor of 1.5 for the U dropouts and 4.7 for the B dropouts. However, the high metal-formation rate at $z > 3.5$ for this model is still at odds with the data (see Ferguson & Babul 1998). Tests with another model show similar results, although the correction factors to go from the FOCAS-measured luminosity density to the luminosity density in the underlying model are not the same.

1. Summary

I have tried in this presentation to give some quantitative insight into how selection effects influence the interpretation of the HDF data. In general, the treatment of the HDF as a flux limited survey is a bad approximation. Magnitudes and radii of galaxies are strongly affected by the measurement techniques (which vary from catalog to catalog) and by the detection algorithm (which is virtually the same in all catalogs generated to date). Faintward of $I_{814} = 27.5$, the angular size distribution of galaxies in the HDF is severely truncated by the survey selection boundaries. Brighter than this, it appears that the HDF galaxies are in general more compact than L^* spirals, but not necessarily more compact than luminous present-day ellipticals. The angular-size distribution is reasonably well matched by a low- q_0 pure-luminosity evolution model (Ferguson & Babul 1998), although such a model does not reproduce the statistics of Lyman-break objects, even when selection effects are accounted for.

The survey selection criteria can have a very strong effect on the statistics of Lyman-break objects, potentially influencing the source counts by an order of magnitude, and the inferred luminosity density by up to a factor of 5. The correction factors depend on the input model.

While this is a fairly discouraging view of quality of information on faint galaxies that can be gleaned from the HDF, nevertheless I think it is fairly accurate. Approximate corrections for some of these selection effects can be derived from the HDF data themselves, but for the most part the magnitude of the selection bias depends on the intrinsic distributions of galaxy sizes and luminosities, which are not well constrained at faint magnitudes. Fortunately, the selection effects are fairly straightforward to model. Comparisons of galaxy evolution models to the HDF really must involve this step.

This work was supported by NASA grant AR-06337, awarded by the Space Telescope Science Institute, which is operated by the Association of Universities for Research in Astronomy, Inc., for NASA under contract NAS5-26555.

REFERENCES

- Coleman, G. D., Wu, C.-C., & Weedman, D. W. 1980, ApJS, 43, 393
- Colley, W., Gnedin, O., Ostriker, J. P., & Rhoads, J. E. 1997, ApJ, 488, 579
- Couch, W. J. 1996, <http://ecf.hq.eso.org/hdf/catalogs/>

- Elson, R. A. W., Santiago, B. X., & Gilmore, G. F. 1996, *New Astron.*, 1, 1
- Ferguson, H. C., & Babul, A. 1998, *MNRAS*, in press
- Flynn, C., Gould, A., & Bahcall, J. N. 1996, *ApJ*, 466, L55
- Gallego, J., Zamorano, J., Aragon-Salamanca, A., & Rego, M. 1995, *ApJ*, 455, L1
- Kron, R. G. 1978, PhD Thesis, University of California at Berkeley
- Lanzetta, K. M., Yahil, A., & Fernandez-Soto, A. 1996, *Nature*, 381, 759
- Lilly, S. J., Le Fevre, O., Crampton, D., Hammer, F., & Tresse, L. 1995, *ApJ*, 455, 50
- Madau, P., Ferguson, H. C., Dickinson, M., Giavalisco, M., Steidel, C. C., & Fruchter, A. S. 1996, *MNRAS*, 283, 1388
- Metcalf, N., Shanks, T., Campos, A., Fong, R., & Gardner, J. P. 1996, *Nature*, 383, 236
- Petrosian, V. 1976, *ApJ*, 209, L1
- Ratnatunga, K. 1996, private communication
- Ratnatunga, K., Griffiths, R., & Ostrander, E. 1997, in preparation
- Williams, R. E., et al. 1996, *AJ*, 112, 1335

Table 1. Selected HDF Catalogs

Catalog	Comments
Couch	SExtractor 1683 Objects on WF chips, selected in F814W. Isophotal limit $\mu_{814} = 26.1$ in 0.016 arcsec^2
Lanzetta et al.	SExtractor 1925 Objects on WF chips, selected in separate bands Isophotal limit $\mu_{814} = 26.2$ in 0.048 arcsec^2
Williams et al.	modified FOCAS 3086 Objects selected in F814W+F606W summed image Isophotal limit $\mu_{814} = 27.5$ in 0.04 arcsec^2
Metcalfe et al.	Detection algorithm described in Metcalfe et al. 1991 3700 Objects Thresholds not specified, but probably the deepest.

Table 2. Model vs. Data for HDF Lyman Break Objects

Data set	Number of U dropouts	Total V_{606}	$\dot{\rho}_Z$	Number of B dropouts	Total I_{814}	$\dot{\rho}_Z$
Input model	62	21.15	4.9×10^{-4}	232	19.14	50×10^{-4}
FOCAS	10	21.58	3.3×10^{-4}	21	20.83	10×10^{-4}
HDF	69	21.48	3.6×10^{-4}	14	23.29	1.1×10^{-4}

Fig. 1.— A portion of the HDF, with objects brighter than $V_{606} = 28.5$ from the Couch (1996) catalog marked. Note that there are quite a lot of sources clearly visible below this magnitude limit, many of which appear in the catalogs, but we have not marked them on the images to avoid clutter. “Total” F606W AB magnitudes are marked for a few galaxies to give an indication of the agreement between catalogs.

Fig. 2.— Same for the Lanzetta et al. (1996) catalog.

Fig. 3.— Same for the Williams et al. (1996) catalog.

Fig. 4.— Same for the Metcalfe et al. (1996) catalog.

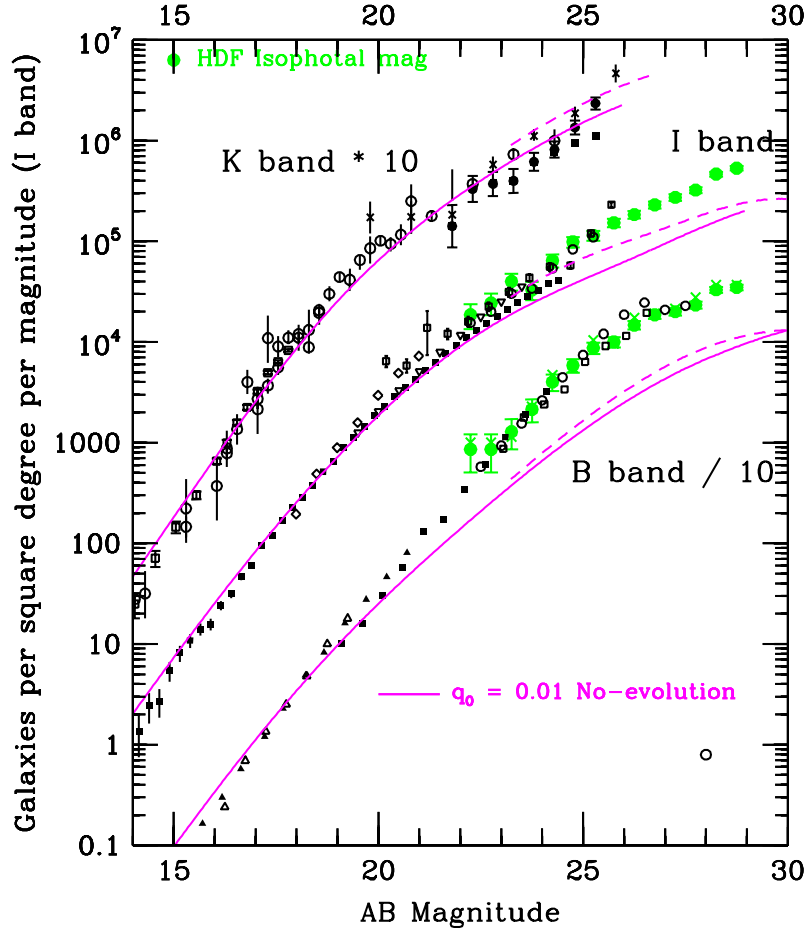


Fig. 5.— HDF counts from Williams et al. (1996), together with a compilation of counts from ground-based surveys. The solid curves show a non-evolving model with $q_0 = 0.01$. The dashed curves show the same model, but with overcounting included. For magnitudes $22 < m_{AB} < 30$, the counts have been multiplied by $1 + (30 - m)/4$, and the magnitudes have been increased by $2.5 \log(1 + (30 - m)/4)$. This illustrates the fairly modest affect that splitting and merging algorithms have on the ability to model galaxy number counts.

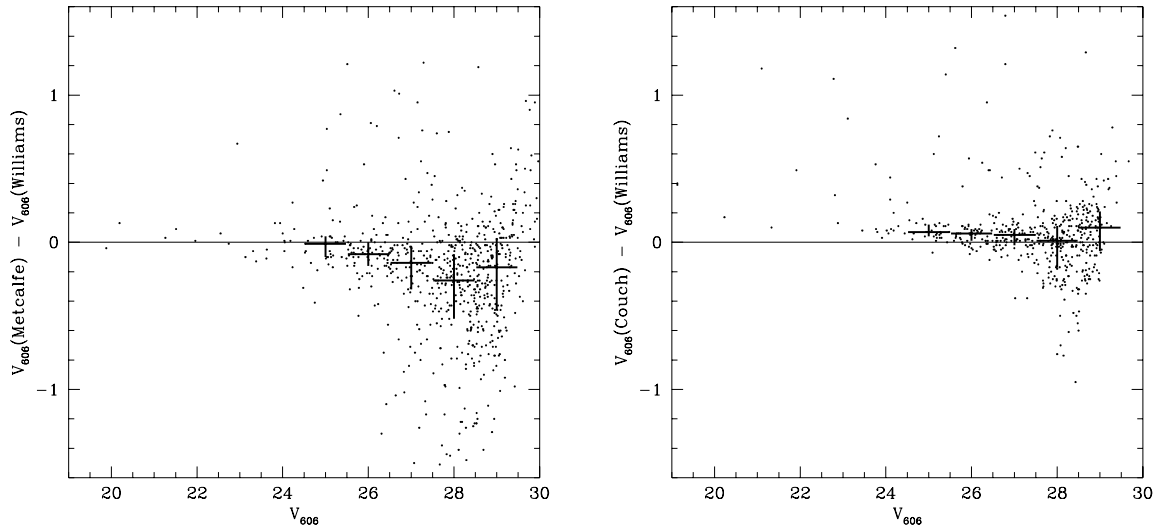


Fig. 6.— The left panel shows a comparison of V_{606} total magnitudes from the Metcalfe et al. and Williams et al. HDF catalogs for galaxies on WF2. The points with error bars show the median and first and third quartiles of the distribution of the residuals in intervals of 1 magnitude. The right panel compares the Williams et al. and the Couch magnitudes.

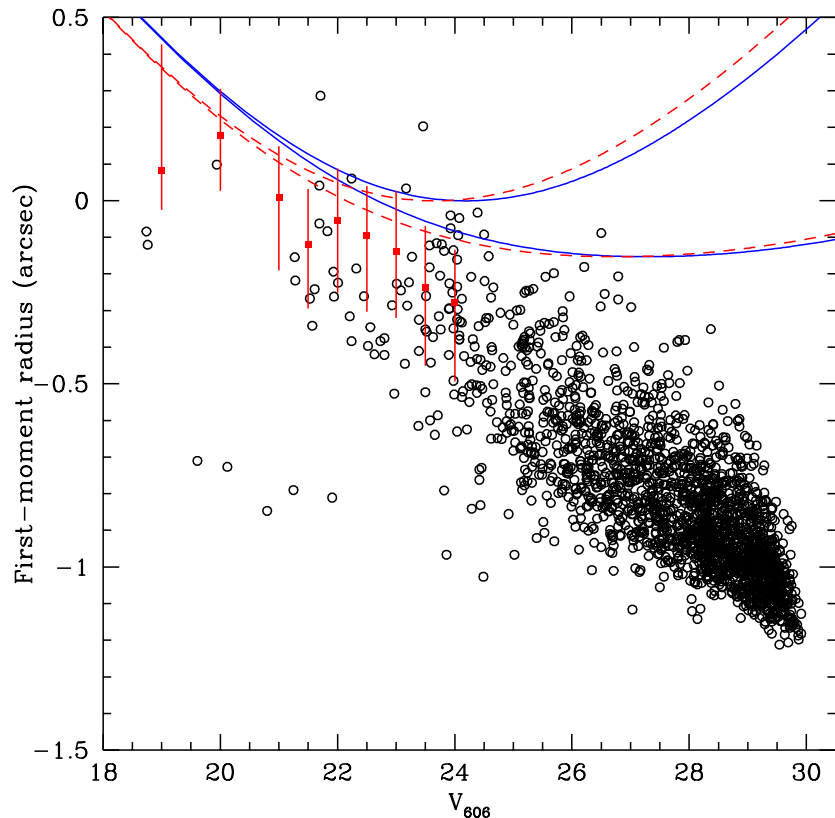


Fig. 7.— Radius–magnitude relations for galaxies in the HDF Williams et al. (1996) catalog (points) and the MDS (points with error bars). The MDS distribution was derived from the catalogs on the MDS web site. The curves show the behavior for non-evolving L^* spirals (solid curves) and ellipticals (dashed curves). The upper pair of curves is for $q_0 = 0.5$; the lower is for $q_0 = 0.01$. *These curves do not take into account selection biases.* The severity of the biases can be seen in the next two figures.

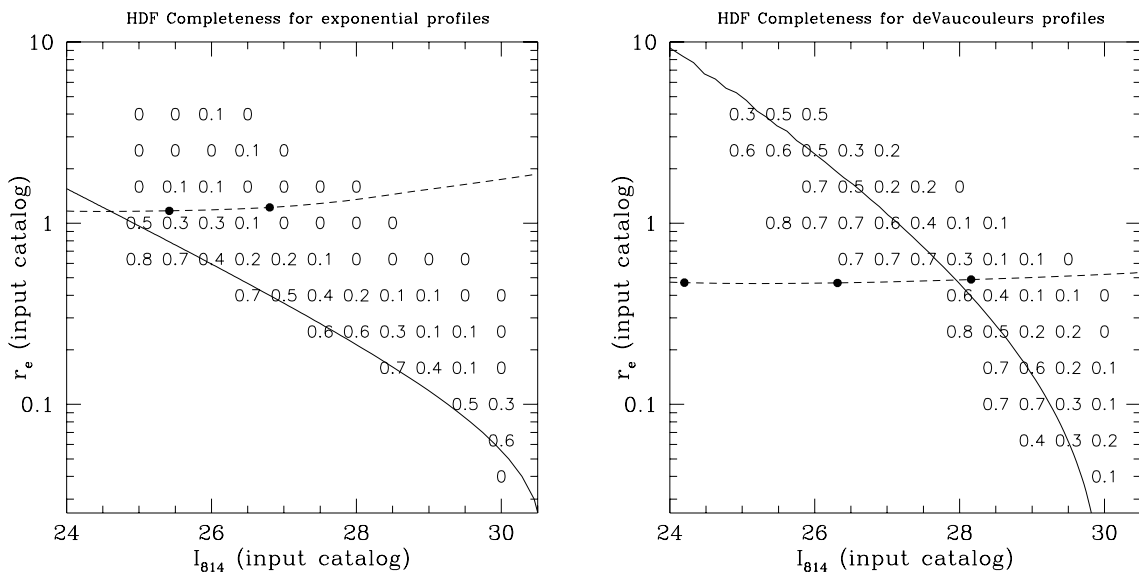


Fig. 8.— Empirical selection boundary for the HDF as a function of half-light radius and total I_{814} magnitude input to the simulations. The left panel shows the limits for face-on galaxies with pure exponential profiles. The right panel shows the same for face-on galaxies with $r^{1/4}$ deVaucouleurs profiles. As there were typically 20 galaxies per bin in the input sample, these estimates are subject to small-number statistics. The solid curves show an analytical model of the FOCAS selection criteria, where we have assumed that a galaxy will be detected if it is brighter than $I_{814} = 30.6$ within a radius of 0.064 arcsec. The dashed curves show the relation between r_e and I_{814} for non-evolving galaxies with $M_B = -21.1$, for $H_0 = 50 \text{ km s}^{-1} \text{ Mpc}^{-1}$, and $q_0 = 0.5$. We have assumed a scale-length $\alpha = 6 \text{ kpc}$ for the spiral, and $r_e = 4 \text{ kpc}$ for the elliptical, and have adopted spectral-energy distributions from Coleman, Wu, & Weedman 1980. The solid dots on the curves for both galaxies correspond to $z = 1, 1.5$, and 2 (from left to right); the $z = 1$ point for the spiral is just off the left of the plot at $I_{814} = 23.7$.

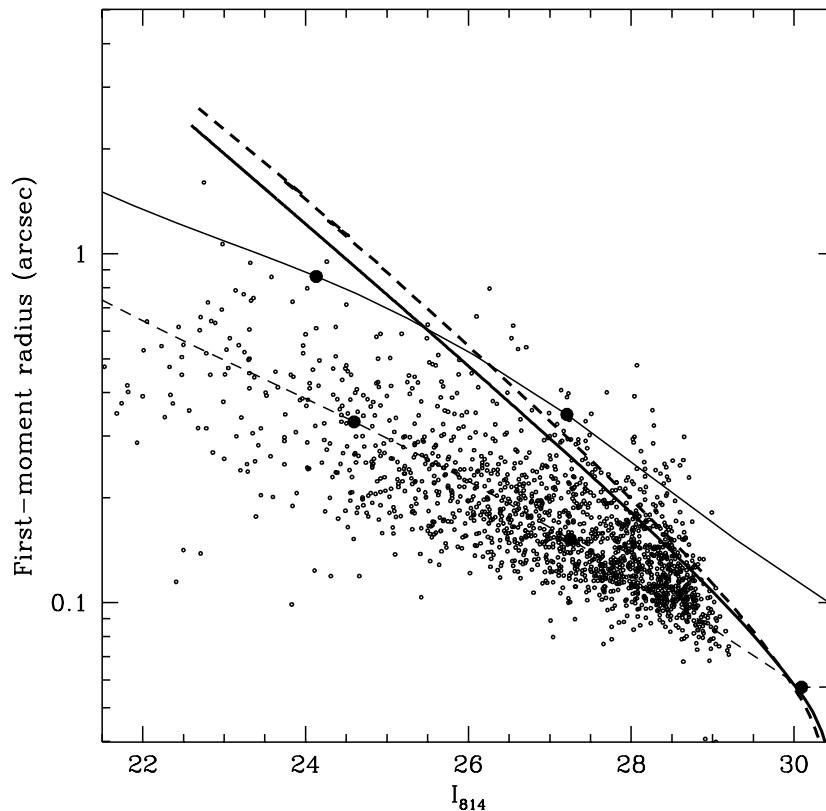


Fig. 9.— HDF angular-size – magnitude relation. Sizes are the first-moment radii and magnitudes are FOCAS I_{814} isophotal magnitudes. The thick lines show the selection boundaries for spirals (solid line) and ellipticals (dashed line), with the same assumptions used for Figure 4. The thin lines show the fiducial non-evolving L^* spiral and elliptical galaxies. The solid dots on the curves for both galaxies correspond to $z = 1, 1.5,$ and 2 (from left to right; the first dot for the spiral is off the plot).

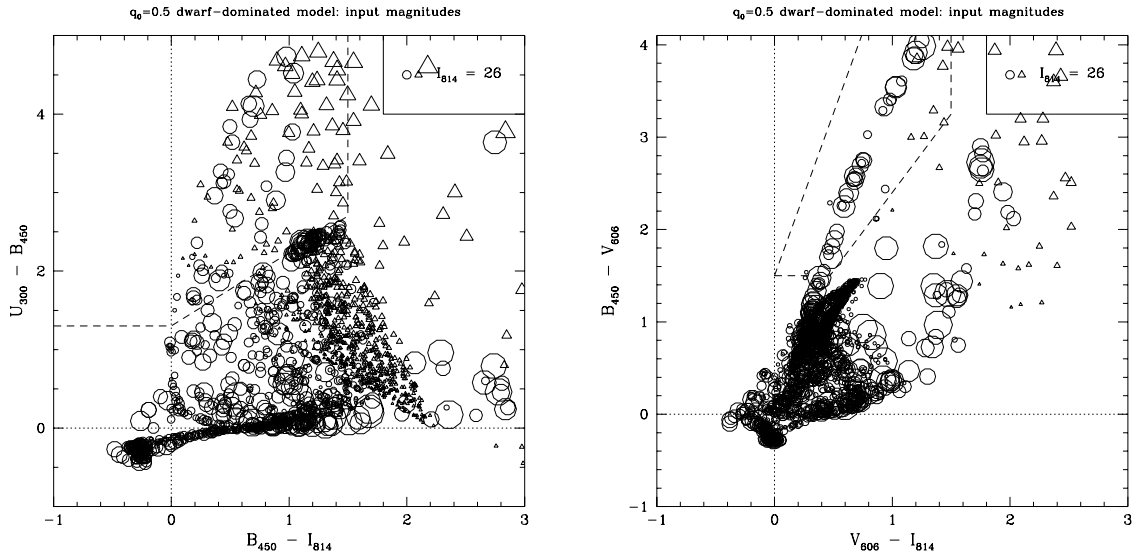


Fig. 10.— Color-color diagrams fashioned after Madau et al. for galaxies in the $q_0 = 0.5$ dwarf-dominated model of Ferguson & Babul 1998. The positions of the galaxies in this diagram are determined from the *true total magnitudes* of the input model. The number of Lyman-break objects within the dashed boundaries should be compared to the next figure, where the same galaxies have been placed in simulated images and measured using FOCAS with the Williams et al. (1996) parameters.

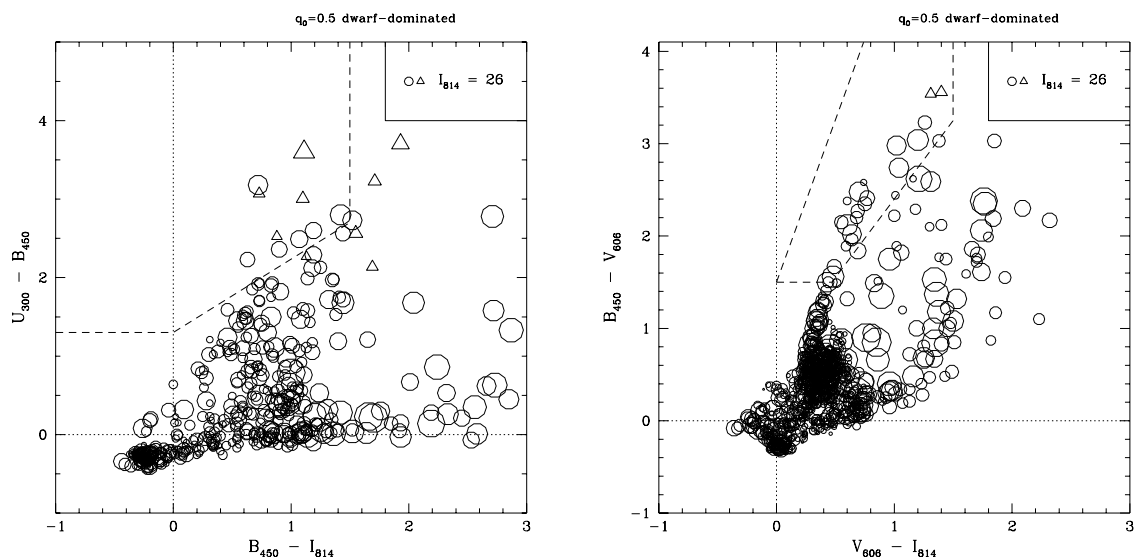


Fig. 11.— Same as the previous figure, but for galaxies measured using FOCAS (with the same parameters used by Williams et al.) in simulated HDF images. Only about 10% of the Lyman-break objects in the input model are recovered by FOCAS. There are various reasons for this. Many of the galaxies that look bright in Fig. 10 have large scale lengths, and hence have FOCAS isophotal magnitudes that are much fainter than their model total magnitudes. In other cases, the FOCAS photometric errors change the colors enough to move the galaxy outside the selection boundary.

This figure "fig1.jpg" is available in "jpg" format from:

<http://arxiv.org/ps/astro-ph/9801058v1>

This figure "fig2.jpg" is available in "jpg" format from:

<http://arxiv.org/ps/astro-ph/9801058v1>

This figure "fig3.jpg" is available in "jpg" format from:

<http://arxiv.org/ps/astro-ph/9801058v1>

This figure "fig4.jpg" is available in "jpg" format from:

<http://arxiv.org/ps/astro-ph/9801058v1>